Available online at www.sciencedirect.com

ScienceDirect

Procedia CIRP 66 (2017) 317 – 322

www.elsevier.com/locate/procedia

1st Cirp Conference on Composite Materials Parts Manufacturing, cirp-ccmpm2017

Material extrusion of continuous fiber reinforced plastics using commingled yarn

T.H.J. Vaneker*

University of Twente, Drienerlolaan 5, 7522 NB Enschede, The Netherlands

* Corresponding author. Tel.: +31-52-4892472; fax: +31-52-4893631. *E-mail address:* t.vaneker@utwente.nl

Abstract

At the University of Twente research has been executed on Additive Manufacturing using continuous fibers based material extrusion. A pultrusion based process has been developed to transform readily available commingled yarn to a polypropylene (PP) E-glass filament. A deposition device has been developed that among others includes a novel low cost fiber cutting device and a modified deposition strategy. Test samples were printed with a flexural modulus of 800% compared to 100% PP samples. Further void percentages up to 20% were found in the printed test samples. Future reduction of this void percentage will further increase the obtainable flexural modulus.

Peer-review under responsibility of the scientific committee of the 1st Cirp Conference on Composite Materials Parts Manufacturing

Keywords: Rapid prototyping, Fiber reinforced plastic, Continuous fiber;

1. Additive manufacturing using fiber reinforced plastics

Additive manufacturing (AM) is the name of a group of processes that are able to produce very complex geometries at low labor and production costs. To establish this the desired part geometry is approximated by subdividing the shape in many 2D layers; more layers ensure better product quality but also increases production time. AM machines produce these layers one by one. The tool that shapes/deposits the material is positioned above (or below) the layer that is produced. As the tool can move freely to any position, the theoretical complexity that can be achieved within a layer, and with that within the product, is theoretically unlimited. Also, as the movement of the tool is not obstructed by the product, the work preparation process, from the 3D design of the product to the control of the production machines, is relatively straightforward and can be 100% automated. These characteristics are among the main benefits that have ensured the recent grow of interest in AM [1]. Some of the drawbacks that have been reported for AM processes are the high surfaces roughness's that stem from the layered building approach, the relatively low production speeds, the high building cost for non-complex parts, the limited freedom in material selection when compared to other manufacturing techniques and the relatively low strength of parts produced with AM techniques [1].

Fiber reinforced plastics are more and more used when among others a high strength to weight ratio is needed (aerospace, automotive). Classic processes for part production using continuous fiber reinforced plastics use mold and mandrel based processes like compression molding, mandrel wrapping, filament winding and wet layup. In general, these processes are labor intensive and restrictive in the geometries that can be obtained. Less labor intensive process variants like Automated tape laying (ATL) and automated fiber placement (AFP) use robots but still to place the fiber/matrix sheets into molds. Currently no classic production processes for continuous fiber reinforced plastics exits that share the benefits of additive manufacturing (automated production of complex products at low costs). Based on shared characteristics like material type, deposition and material fusion methodology used, the ASTM (American Society for Testing and Materials) in 2010 has defined 7 AM process groups [2]. None of these

Peer-review under responsibility of the scientific committee of the 1st Cirp Conference on Composite Materials Parts Manufacturing
doi:10.1016/j.procir.2017.03.367

groups have composite materials and products as their common denominator, although some have process or material variants that use additives to enhance properties of the finalized product. Based on that observation it can be concluded that there is a need for the development of AM processes using continuous fibers for products that are geometrically complex and for which the functionality can be characterized by high strength, high stiffness and low weight.

2. State of the art in AM with continuous fibers

When fibers are used in AM these additives fibers are often used to enhance the mechanical, electrical or thermal properties of parts [3]. On a high level of abstraction 3 strategies can be identified in which fibers are used to produce parts that have mechanical properties that surpass those of the base materials. These strategies themselves are often applicable within several of the 7 AM process groups.

1. Short, chopped fibers are often mixed in with existing AM materials to increase mechanical strength of the resulting parts. These fibers are included in processes like Fused deposition modeling (FDM), Stereo lithography (SLA), Selective Laser Sintering (SLS) etc. Tensile strength improvements up to 194% are obtained using chopped fiber additions [3].
2. It is also possible to directly use fiber reinforced sheets to build 3D products. Impossible objects [4] has developed a process on which inkjet technology is used to print polymers on sheets of fibers. After stacking and oven consolidation a mechanical or chemical process is used to remove the unwanted uncoated fibers; the desired part geometry remains. A tensile strength increase by a factor 10 is reported by the company [4].
3. Finally, AM parts can also be reinforced with continuous fibers. Research focusing on these processes are discussed in more detail in the next subchapter.

2.1. State of the art in AM part reinforcement with continuous fibers.

In recent years some research has been conducted that focused on development and characterization of new methods for additive manufacturing based production of complex geometries with continuous fibers reinforcement.

Melenka [5] studied the elastic behavior of test specimen printed with the commercially available MarkOne 3D printer from Markforged [6]. This printer creates the base geometry in Nylon while 3 reinforcement options are available; Carbon Fiber, Fiberglass and Kevlar. The printing/reinforcement strategy used is printing parts while adding concentric rings of fibers that follow the components outer geometry. Tensile test samples were printed using Kevlar reinforcements. The geometry of the samples limited the number of concentric rings that could be printed to a maximum of 5, which in its turn limited the maximal volume fraction of fibers to be used. The experimentally determined elastic modulus was found to be 1.7, 6.9 and 9.0 GPa for Kevlar volume fractions of 4.0, 8.1 and 10.1% respectively. In these tests it was observed that the location of the start of the filament placement was also the location of failure during testing. This might be explained by the limited number of concentric rings and thus the relatively large effect of this local distortion.

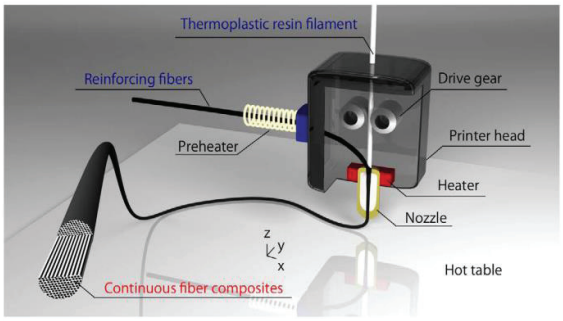

Fig. 1. 3D printing device as developed and used by Matsuzaki et al.[8]. To increase printing flexibility, it uses two separate material strands that are joined in the heater of the extrusion head.

Klift et al. [7] also used the MarkOne [6] to study the effect of fiber reinforcement on the mechanical properties of plastic parts. The printed tensile test specimens had a carbon fiber volume fraction of 1.0% in a nylon matrix material. The resulting mechanical properties were lower than expected according to the rule of mixing used for composites. These low mechanical properties were contributed to the delamination of the layers and the formation of voids during deposition. Some solutions were suggested to prevent these problems from happening (preheating of the carbon fibers, changing the temperature of the print bed, decreasing the diameter of the nozzle) but not validated.

Matsuzaki et al. [8] developed a non-commercial variant of the FDM material extrusion process where both the reinforcement and the matrix material are fed into the extruder as separate material flows (fig. 1). Experiments focused on testing both carbon and natural fibers (jute) as reinforcement while using Polylactic Acid (PLA) as the matrix material. For both fiber types an increase in the mechanical properties was observed. The tensile modulus (19.5 GPA, +599%) and strength (185.2 MPA, +435%) of the carbon fiber reinforced specimen (6.6% volume fraction fibers) are significantly higher when compared to 100% PLA samples. Also 3-point bending tests were executed, but the results were estimated to be questionable, as the distribution of the fibers was non-uniformly over the cross section.

Li et al. [9] and Tian et al. [10] conducted experiments similar to Matsuzaki [8], as they used separate material bundles (Carbon fiber and PLA matrix material) to create test samples. Li [9] created test samples with 34 volume % fibers. As expected a significant increase in tensile strength (80 MPA; 185%) was found. The increase in flexure strength was only limited (59 MPA; 11%), which was contributed to the poor adhesion between PLA and carbon fibers. A second set of tests were conducted for which the surface of the carbon fibers was modified to increase the strength of the bonding interface between the PLA and the fibers. These samples showed significant increases in both tensile (225%) and flexural strength (194%) when compared to 100% PLA test specimen.

Tian [10] investigated the process settings to define optimal printing characteristics. For relatively high nozzle temperatures, low layer thicknesses and low hatch spacing distances the specimen with the best mechanical properties were found. A fiber volume content of 27% resulted in a flexural strength of 335 MPa and flexural modulus of 30 GPa.

3. Methodology

All the research on AM with continuous fibers, as presented in chapter 2, mix the fibers and plastic support material in the extrusion nozzle. This might induce problems, like the adhesion problems mentioned by Li et al.[9].

In this paper a different approach will be presented. The approach described here was developed by Rietema [11] as a continuation of the work of De Bruijn [12]. Major differences in the approach chosen can be found in the basic design of the extrusion mechanism, the material type used, the way the material is fed into the machine and finally the deposition strategy. These topics will be discussed in the remainder of this section. In chapter 4 the findings on the printing results using this approach will be elaborated upon.

3.1. Material used

At the start of research [11],[12] dedicated filament with continuous fiber reinforcement was not available for 3D printers. For this reason, other materials were investigated for their suitability. To keep close to the original design of FDM type 3D printers, an input material that already contained the fiber as well as the matrix material was chosen. Further demands on the material were a high volume fraction of fibers, a round cross section and a small diameter of that cross section (to be able to produce thin layers and complex products). Two possible candidate materials were found suitable and available; both materials needed preprocessing to come to the required circular cross section.

- De Bruijn [12] conducted experiments with a material produced by [13]. It has dimensions of 5 x 0.5 mm and a 54.8 m% E-glass content. Pre-processing and extrusion would be combined during extrusion of the material/filament. During reshaping the material to round filament a theoretical diameter of 1.78 mm could be obtained.
- The second material investigated [11] is a commingled yarn of E-glass and Polypropylene filaments, TWINTEX® RPP60N265. It was manufactured by FiberGlass Industries* [14], has a linear mass of 1870 Tex [gr/km] and a 60 m% E-glass content. After consolidation a theoretical diameter of 1.26 mm is achievable.

Both materials use PP as matrix material, which is less suitable and less used for FDM based processes but were still chosen based on availability. Based on the obtainable diameter of the filament TWINTEX® was chosen as the input material for this project.

* This company no longer exists. However, similar yarns are readily available in industry.

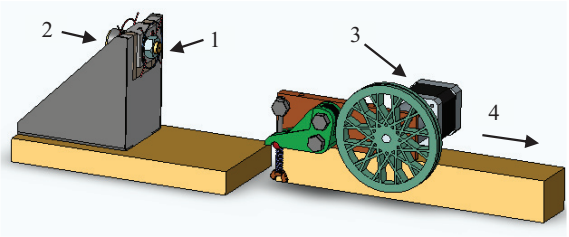

Fig. 2. Pultrusion mechanism. 1 Brass mold for shaping the yarn. 2 Heating device. 3 Pulling motor. 4 Towards a larger wheel for storing the preprocessed yarn.

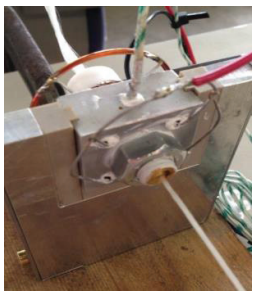

Fig. 3. Detailed view of the mold in the heater with the yarn entering from above and the filament leaving the at the bottom.

3.2. Design of the deposition apparatus

The developed apparatus [11] for continuous fiber deposition differs from the standard FDM equipment on two major facets. Regular FDM 3D printers push the filament trough the heated extruder. A cheap and readily available yarn is chosen as starting material, preprocessing of the yarn is needed to transform the flexible, rope like material into a solid filament. Furthermore, during deposition regular cutting of the yarn is essential to ensure freeform deposition and thus enable the mold-less production of complex fiber reinforced shapes.

3.2.1. Material preprocessing

The pultrusion apparatus developed for preprocessing the yarn contains a brass mold with a central hole with diameter 1.3 mm (fig. 2 and 3). This mold is embedded in a heater of which the temperature is automatically controlled. The pultrusion speed is managed by a servo motor and a filament pull wheel (fig 2 no 3). After this wheel the processed yarn is stored on a larger wheel (a 28 inch bicycle wheel; not displayed in fig. 2), so it can be used as input for subsequent use in the

3D Printer. Both the pultrusion speed as the mold temperature are controlled by an Arduino Uno.

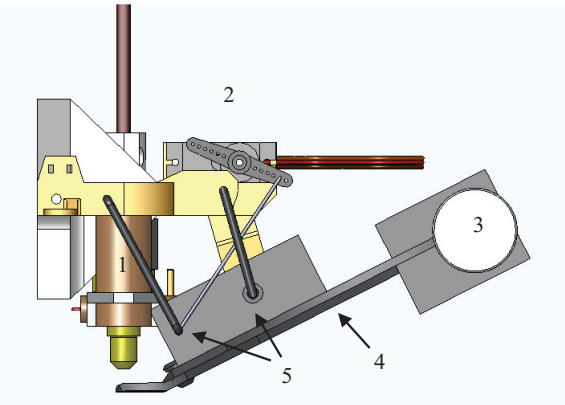

Fig. 4. The design of the cutting device. 1 Filament extrusion head. 2 Servo (TowerPro MG995). 3 Solenoid (Intertec ITS-LZ 2560-Z-6VDC). 4 Cutters 5 4-bar linkage.

3.2.2. The filament cutting device

The ability of 3D printers to create high complex products is directly linked to the ability of the tool to deposit material anywhere in the currently created 2D layer. This freedom of movement of the tool is limited if continuous fibers are used; the filament needs to be cut regularly.

Several cutting mechanism were identified that could be suitable to cut the fibers. Based on the limited budget within the project it was chosen to design and implement an automated wire cutter as depicted in fig. 4. The goal of the cutter is to cut the fiber directly at the top surface of the layer currently deposited. To do so the cutting action involves two distinct movements; the extrusion head moves upwards while the cutter itself moves down and sideways so it can be positioned underneath the extrusion head. To facilitate this movement of the cutter it is attached to a set of beams that together form a 4-bar linkage. The movement of this 4-bar linkage is actuated by a servo (fig 4, no. 2). The actuation of the cutters itself is controlled by a solenoid (fig 4, no. 3).

3.2.3. System integration

The cutter described in the previous paragraph was mounted on an open source RepRap Prusa I3 FDM printer. To ensure that actual deposition could be achieved some modifications to the standard control software of the printer were needed.

- For standard FDM printers the extrusion speed and the movement speed of the extrusion head are independent parameters. As the fibers will not elongate during printing, the extrusion speed is redefined to be equal to the movement speed of the extrusion head.
- The printing script (Slicr3D, [13]) was modified to ensure that the fiber was cut when required. Based on an evaluation of the geometry and the standard G-code (as defined by the Slicer3D software) the following cutting moment were introduced.
  - Cut if the extrusion head moves to a new location while no material is extruded (movement to a new starting position).
  - Cut if the angle (120 degree) between two subsequent lines is larger than a certain threshold.
  - Approximate small radii (< 6 mm) with a few straight lines, with a cut between the lines.

The last two cutting commands were introduced based on generic observations on the quality of the printed material. If the filament is forced into a new direction, the distribution of the fibers within the matrix material is non-uniform (fig. 5).

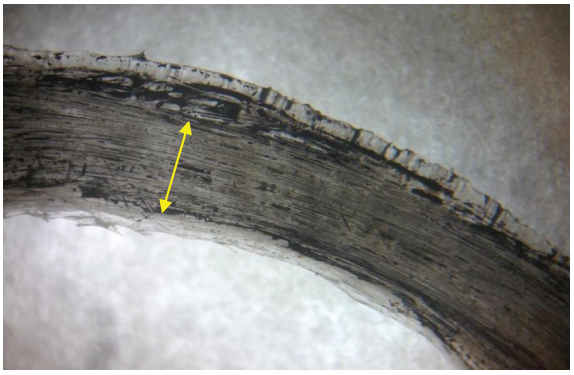

Fig. 5. The effect of bending the filament during extrusion. At the location of the arrow it is shown that the fibres have shifted to one side, compared to the originally, uniformly distributed, position within the filament.

4. Results

4.1. Preprocessing quality

The pultrusion device was optimized to find the optimal processing parameters of the yarn. To do so the temperature of the nozzle was varied between 180°C and 210°C with steps of

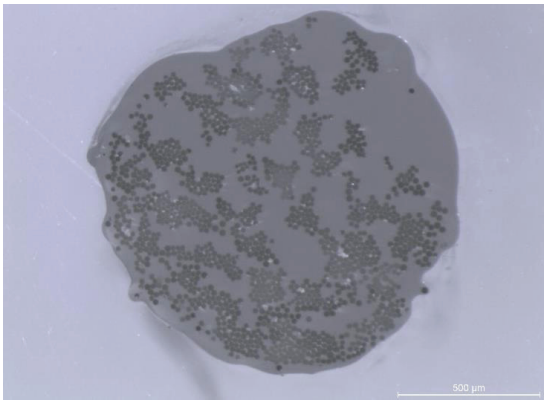

Fig. 6. Filament with fiber distribution for the selected processing parameters (v = 2 m/s, T= 200 °C). Dark grey spots are fibers, medium grey indicates matrix material. Some lighter spots are indicative for voids that are present after the pultrusion process

10°C. For each temperature the pultrusion speed is varied between 0.5 to 3 mm/min with steps of 0.5mm/min. Short

lengths of the obtained 24 samples are inserted in a holder and embedded in epoxy. After 24 hours of curing, the epoxy with filaments is cut in half with a diamond saw and sanded with increasing P-number (P500 to P 4000) and polished to obtain a clear view (fig. 6) on the cross sectional area. Based on an optical inspection of the uniformity of the distribution of the fibers over cross section a pultrusion speed of 2 mm/s and temperature of 200 °C was determined to be optimal.

4.2. Deposition quality.

A total of 10 samples have been printed to investigate the influence of the printing parameters on the quality of the deposited material. The existence and amount of air voids is taken as a measurement of the deposition quality. To determine the existence of air voids the samples are cut in half, embedded in epoxy a polished (up to P6000). Microscopic pictures have been taken and a program for analysis of scientific multidimensional image data [16] is used to evaluate the results.

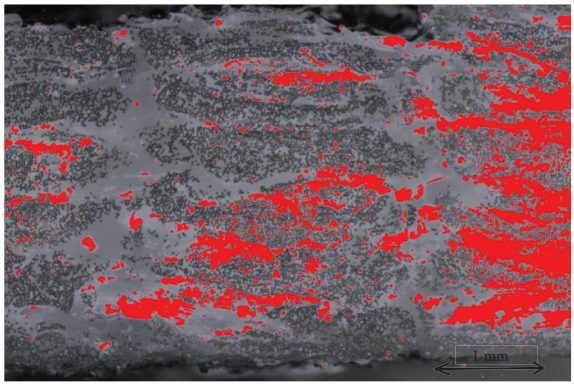

Fig. 7. Automatic determination of air voids for sample 2. The higher threshold is used and air voids have been indicated in red.

After consultation with experts it has been determined that the (originally) lighter area's in the pictures represent the voids. As the lightness of these spots cannot be defined unambiguously, a lower and higher threshold for the determination of air voids has been defined (see figure 7 for the plot of air voids as determined using the higher threshold). Pixels determined to be voids are automatically colored red. The results of the determination process for the voids for all samples is depicted in table 1.

Table 1. Average void percentages in the test samples of table 1. No = sample number. ET = Extrusion Temperature. LH – Layer height. ES = extrusion speed. AV min = Air void estimation lower limit. AV max = air void estimation upper limit.

No	ET (°C)	LH (mm)	ES (mm/min)	AV min (%)	AVMin (%)
1	210	0.5	60	1.4	10.7
2	200	0.5	60	0.9	16.2
3	190	0.5	60	0.6	14.0
4	200	0.5	120	1.5	29.3
5	200	0.5	30	2.0	17.8
6	200	0.4	60	1.6	23.7
7	200	0.6	60	0.9	23.8
8	200	0.8	60	1.3	21.5

From fig. 7 it can be concluded that the concentration of voids tends to be aligned in horizontal lines, implying that the consolidation between subsequent layers was insufficient within this sample. This trend was also observed in the other samples. The consolidation between different lines in the same layer does not result in noticeable vertical lines in the concentration of the voids. Finally, the results presented in table 1 don't present a clear relation between the process settings investigated and the total void percentage found at the cross sections of the samples.

4.3. Determination of the flexural modulus

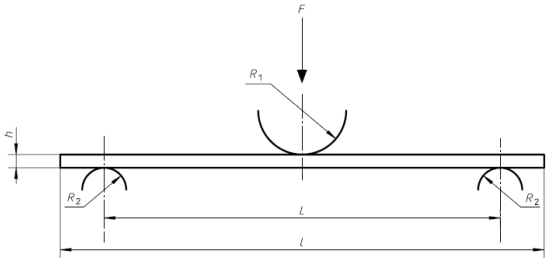

Fig. 8. Design of the 3-point bending test. R_1 = 3.175 mm. R_2 = 1.59 mm. L = 40 mm. The samples used had a length of 60 mm and had a variable height h.

For a 3-point bending test new samples (see table 2) were printed and sanded down to comply with the standards of ISO14125. The layout and dimensions of the test setup are depicted in figure 8. The result of the bending test can be found in table 2.

Table 2. Flexural modulus for the samples of table 2, measured using a 3-point bending tests. No = sample number. ET = extrusion temperature. LH = Layer height. ES = extrusion speed. FM = average flexural modulus for the sample set. SD = standard deviation on the measured values of FM.

No	ET (°C)	LH (mm)	ES (mm/min)	S	FM (GPA)	SD (GPA)
1	200	0.5	90	6	13.00	0.57
2	210	0.5	90	5	12.37	0.76
3	200	0.4	90	3	13.06	0.34
4	200	0.6	90	3	11.44	0.73

From table 2 it can be concluded that the extrusion temperature and layer height have little effect on the measured flexural modulus of the printed samples. The theoretical flexural modulus after processing, 26.5 GPA (as defined by the material supplier [14]) have not been reproduced in these tests. This might be explained by the relatively high void content of the samples (see table 1 for indicative values). Hagstrand [17] has investigated the relation between void percentage and flexural modulus and defined a linear relation (validated up to 14 volume % air voids) between the two parameters. It was stated that for every 1% of air voids the flexural modulus

decreases with 1.5%. For samples with an estimated void content of 19% this would result into a predicted flexural modulus of 18.9 GPA.

The actual concentration of the voids over the cross section, see figure 9, might be an explanation of the further discrepancy between the predicted (18.9 GPA) and the measured (average 12.8 GPA over all samples) flexural modulus. The uneven distribution of the voids over the cross section result in larger holes, what might explain the lower average flexural modulus.

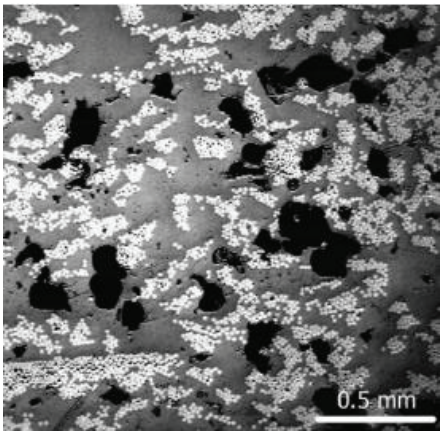

Fig 9. Cross section a sample showing uneven distribution of voids to form holes (black)

4.4. Test of the deposition strategy.

To test the deposition strategy implemented a basic shape has been printed. This shape is displayed in figure 10.

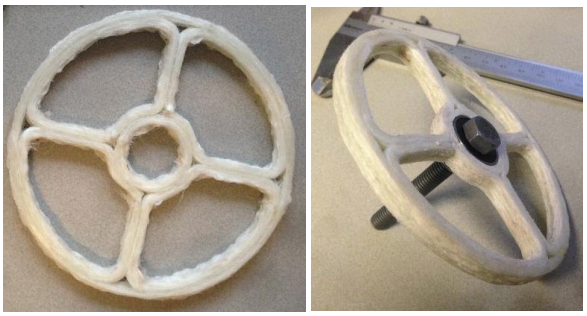

Fig 10. 3D printed structure. The structure on the left shows a high surface roughness, mainly due to unbound fibers at the surface of the structure. The surface quality was manually improved for the right picture

5. Conclusion and future work

A novel approach to additive manufacturing with continuous fiber reinforcement was presented. The approach has major differences is the material used, conmingled yarn, which also affects the material extrusion and deposition process. As a result, the overall deposition apparatus more closely relates to the standard extrusion process found in every day FDM printers.

Relative high percentages of voids were observed in the printed specimen, although no direct relation was found between variations in the void percentage and the process parameters used. Probably as a result of the high void percentage the resulting flexural modulus was found to be only 48% of the theoretically possible values.

Future work will focus on the reduction of the void percentage in the printed samples. Next to the processing parameters the consolidation pressure will be investigated and optimized as a means to reduce this percentage. Also processing conditions for the extrusion of a secondary deposition material, not fiber reinforced, will be investigated. This promises to increase the possible complexity of the parts to be produced.

Acknowledgements

This work is reports of a continuous line of research at the University of Twente, the Netherlands. Special thanks goes to Thomas de Bruijn and Menno Jan Rietema, as this paper is to a large extend based upon their master thesis reports.

References

[1] Thompson M.K., Moroni G., Vaneker T. et al., Design for Additive Manufacturing: Trends, opportunities, considerations, and constraints. CIRP Annals - Manufacturing Technology, DOI: 10.1016/j.cirp.2016.05.004. 2016.
[2] American Society for Testing Materials. ASTM F2792-12a. Standard Terminology for Additive Manufacturing Technologies. DOI: 10.1520/F2792-12A, 2010.
[3] Wang et al. 3D printing of polymer matrix composites: a review and prospective. Composites part B 110. Pages 442 – 458. 2017.
[4] http://impossible-objects.com/. Visited online 12 -1-2017
[5] Melenka et al. Evaluation and prediction of the tensile properties of continuous fiber-reinforced 3D printed structures. Composite Structures 153, pages 866–875, 2016
[6] Makerforged. https://markforged.com/ Visited online January 2017.
[7] Klift van der F., et al. 3D Printing of Continuous Carbon Fibre Reinforced Thermo-Plastic (CFRTP) Tensile Test Specimens. Open Journal of Composite Materials, DOI: 10.4236/ojcm.2016.61003, 2016
[8] Matsuzaki et al. Three-dimensional printing of continuous-fiber composites by in-nozzle impregnation. Nature Science reports. 6:23058. DOI: 10.1038/srep23058. 2016
[9] Li N., Li Y., Liu, S., Rapid prototyping of continuous carbon fiber reinforced polylacticacid composites by 3D printing. Journal of Materials Processing Technology 238, pages 218–225, 2016
[10] Tian X., Liu T., Yang C., Wang Q., I D., Interface and performance of 3D printed continuous carbon fiber. Composites: Part A 88, Pages 198–205, 2016
[11] Rietema. M.J. Design of a prototype machine for 3D printing with continious fibre reinforcement. Master thesis University of Twente. https://essay.utwente.nl. 2015
[12] Bruijn de. Developing a process for continious fibres in Fused Depostion modelling. Master thesis University of Twente. https://essay.utwente.nl. 2013
[13] http://compositetape.com/ [Accessed 10 Janurary 2014].
[14] http://fiberglassindustries.com/twintex.htm. [Accessed 5 april 2014].
[15] http://slic3r.org/ [accesed 12 january 2017]
[16] Schindelin J., "Fiji: an open-source platform for biological-image analysis," Nature methods, vol. 9, no. 7, pp. 676-682, 2012.
[17] Hagstrand, "The influence of void content on the structural flexural performance of unidirectional glass fibre reinforced polypropylene composites," Composites, vol. Part A, no. 36, p. 705–714,